Biochimica et Biophysica Acta, 1147 (1993) 154–160

BBAMEM 75944

A microscopic model for lipid/protein bilayers with critical mixing

Zhengping Zhang [a], Maria M. Sperotto [c], Martin J. Zuckermann [a] and Ole G. Mouritsen [b,c]

[a] *Centre for the Physics of Materials, Department of Physics, McGill University, Montréal, Québec (Canada),* [b] *Canadian Institute of Advanced Research, Vancouver (Canada) and* [c] *Department of Physical Chemistry, The Technical University of Denmark, Lyngby (Denmark)*

(Received 13 October 1992)

Key words: Lipid bilayer; Polypeptide; Phase diagram; Critical mixing; Gramicidin A

A statistical mechanical lattice model is proposed to describe the phase diagram of phospholipid bilayers with small transmembrane proteins or polypeptides. The model is based on the extended Pink-Green-Chapman model (Zhang et al. (1992) Phys. Rev. A 45, 7560–7567) for pure lipid bilayers which undergo a first-order gel–fluid phase transition. The interaction between the lipid bilayer and the protein or polypeptide is modelled using the concept of hydrophobic matching. The phase diagram has been derived by computer-simulation techniques which fully account for thermal density fluctuations and which operate on the level of the free-energy thereby permitting an accurate identification of the phase boundaries. The calculations predict a closed loop of gel–fluid coexistence with a lower critical mixing point. Specific-heat traces across the phase diagram are also presented. The theoretical results for the phase diagram, the specific-heat function, and the transition enthalpy are related to recent experimental measurements on phospholipid bilayers mixed with synthetic transmembrane amphiphilic polypeptides or with gramicidin A.

I. Introduction

Insertion of transmembrane amphiphilic proteins or polypeptides into lipid membranes is known to have a considerable influence on the phase equilibria of the mixed system [1]. In particular the lipid–protein interactions often induce dramatic phase-separation phenomena. Moreover, the aggregation state of the proteins within the different lipid phases is strongly influenced by the interactions with the lipid bilayer. Despite an intensive experimental activity on lipid–protein interactions in recent years [2] only a few phase diagrams of lipid/protein mixtures have been worked out with sufficient accuracy to allow a closer theoretical interpretation in terms of fundamental forms of the lipid–protein interactions. One of the theoretical guidelines which has been proposed to relate protein-induced lipid-bilayer phase equilibria to basic physical properties of the lipid/protein interfacial contact is the concept of hydrophobic matching [3,4] between the lipid-bilayer and protein hydrophobic thicknesses. This concept has had some success in predicting phase diagrams for lipid bilayers reconstituted with proteins like bacteriorhodopsin, photosynthetic reaction center proteins, as well as band 3 protein [1]. In this paper we explore the use of hydrophobic matching to predict phase diagrams for DPPC bilayers incorporated with small protein-like molecules, such as amphiphilic transmembrane polypeptides of the type Lys_2-Gly-Leu_n-Lys_2-Ala-amide as well as gramicidin A. By using a microscopic interaction model we show that the effect of mismatch between the hydrophobic thickness of the lipid bilayer in its gel and fluid phases and the hydrophobic length of the polypeptide leads to a closed gel–fluid coexistence loop and a lower critical mixing point in good agreement with experimental data [6,7].

The difficulty in obtaining an accurate experimental phase diagram for lipid/protein and lipid/polypeptide mixtures is related to several different circumstances. Firstly, most experiments do not yield the free energy of the mixture but rather certain derivatives of the free energy, such as specific heat and various spectroscopic order parameters. It is often difficult to determine the position of phase boundaries based on these deriva-

Correspondence to: O.G. Mouritsen, Department of Physical Chemistry, The Technical University of Denmark, Building 206, DK-2800 Lyngby, Denmark.

Abbreviations: DMPC, dimyristoylphosphatidylcholine; DPPC, dipalmitoylphosphatidylcholine; EPR, electron paramagnetic resonance; NMR, nuclear magnetic resonance; DSC, differential scanning calorimetry.

tives without invoking certain model assumptions. As an example, apparent anomalies in the specific heat are not sufficient conditions for the presence of a phase transition or a phase boundary, and spectroscopic order parameters refer in principle to certain intrinsic time and length scales of the experimental technique in question. Specifically, a superposition of two different spectra need not imply a thermodynamic phase separation but only that the spectroscopic probes with a given diffusional time constant 'see' two different environments over the time scale of the experiment. This implies that determinations of phase diagrams using experimental techniques such as NMR or EPR in principle tend to place the phase boundaries too far into the thermodynamic one-phase regions. Due to the shorter timescale, the EPR determination of the phase diagram will be the less reliable.

In the present paper we present accurate numerical results for the phase diagram of a model of lipid/protein mixtures. We simultaneously calculate specific-heat traces across the phase diagram for the same model. The model assumes that the lipid–protein interactions are controlled by the hydrophobic mismatch condition. The thermodynamic properties of the model are determined by Monte Carlo simulation techniques [8] taking proper account of the density fluctuations near the phase transitions which are important for calculating the specific heat accurately. The simulations also treat the entropy of mixing correctly. The computer-simulation data have been analyzed on the level of the free energy which permits a direct identification of the phase boundaries using standard thermodynamics. Our work is therefore complementary to earlier theoretical work on lipid–protein phase equilibria, e.g., the phenomenological modelling of critical mixing by Morrow and Whitehead [9] which does not allow for thermal density fluctuations and the microscopic modelling by Pink and Chapman [10] who treated the lipid–protein interactions in a non-specific fashion. The microscopic model and the calculational techniques are described in Section II and the results for the phase equilibria and the specific heat are presented in Section III. Finally, the results are discussed in Section IV in relation to experimental measurements on phospholipid bilayers incorporated with small α-helical synthetic, amphiphilic polypeptides and with gramicidin A.

II. Microscopic model and calculational techniques

Microscopic model

The microscopic interaction model used in the present paper to describe a lipid bilayer mixed with small transmembrane proteins or polypeptides consists of two parts. The first part, $\mathscr{H}_{LL}$, describes the internal energy of the pure lipid bilayer and the second part, $\mathscr{H}_{LP}$, describes the interactions between the lipid bilayer and the protein. Direct interactions between different proteins are neglected since we shall only be concerned with low protein/lipid ratios. The pure lipid bilayer is described by the extended Pink-Green-Chapman model [11]

$$\mathscr{H}_{LL} = \sum_{i}\sum_{\alpha=1}^{10}(E_\alpha + \Pi A_\alpha)\mathscr{L}_{\alpha,i} - \frac{J_0}{2}\sum_{\langle i,j\rangle}\sum_{\alpha,\beta=1}^{10} I_\alpha I_\beta \mathscr{L}_{\alpha,i}\mathscr{L}_{\beta,j} + \frac{\gamma_{mis}^{LL}}{2}\sum_{\langle i,j\rangle}\sum_{\alpha,\beta}|d_\alpha - d_\beta|\mathscr{L}_{\alpha,i}\mathscr{L}_{\beta,j} \quad (1)$$

The first two terms in Eqn. 1 correspond to the standard Pink-Green-Chapman model [12], which is a ten-state model accounting for the van der Waals interactions between the lipid acyl chains as well as the conformational statistics of the chains. $\langle i,j\rangle$ are nearest neighbor indices on a triangular lattice on which the lipid acyl chains are placed. J_0 is the strength of the van der Waals interaction and $\mathscr{L}_{\alpha,i}$ is an occupation variable which is unity when the ith chain is in the αth conformational state and zero otherwise. I_α is a product of a term related to the van der Waals interaction between chains and a phenomenological expression for the shape-dependent nematic order parameter for the chain conformations. Π represents the effective lateral pressure exerted on a lipid bilayer due to interfacial effects (hydration, polar head interactions etc.). The parameters J_0 and Π were determined earlier by fitting to experimental values for the transition temperatures and transition enthalpies of pure saturated PC bilayers [8]. The values found for dipalmitoyl phosphatidylcholine (DPPC) are $J_0 \approx 0.71 \cdot 10^{-13}$ erg and Π = 30 dyne/cm. The extension of the Pink-Green-Chapman model consists in adding the third term in the Hamiltonian in Eqn. 1. This term, which describes a mismatch interaction between different conformational states of the acyl chains, was introduced in Ref. 11 to bring the Pink-Green-Chapman model into a region of first-order transitions of the pure lipid bilayer. The mismatch interaction is formulated in terms of a geometric variable, d_α, which is the hydrocarbon chain length for the αth conformational state. d_α is directly related to the value of the acyl-chain cross-sectional area, A_α, since the volume of an acyl chain is assumed to be invariant under temperature changes. The parameter γ_{mis} is related to the hydrophobic effect.

The lipid–protein interactions, $\mathscr{H}_{LP}$, can now be formulated in terms of a direct lipid–protein interaction in addition to a hydrophobic mismatch term [13,14]

$$\mathscr{H}_{LP} = \Pi A_P \sum_i \mathscr{L}_{P,i} - \frac{J_{LP}}{2}\left(\frac{d_P}{d_l}\right)\sum_{\langle i,j\rangle}\sum_{\alpha} I_\alpha \mathscr{L}_{\alpha,i}\mathscr{L}_{P,j} + \frac{\gamma_{mis}^{LP}}{2}\sum_{\langle i,j\rangle}\sum_{\alpha}|d_\alpha - d_P|\mathscr{L}_{\alpha,i}\mathscr{L}_{P,j} \quad (2)$$

The protein is characterized by a cross-sectional area, A_P, and a half-length of the hydrophobic core, d_P. d_l is the lipid acyl-chain length in the all-*trans* conformation. It is assumed in this description that the hydrophobic membrane-spanning part of the protein molecule is a stiff, rod-like, and hydrophobically smooth object without appreciable internal flexibility. It is also assumed that the protein is small in the sense that it only occupies one site of the lipid lattice. This assumption, which is made for computational convenience, will be discussed further in Section IV. The parameter γ_{mis}^{LP} is related to the hydrophobic effect describing the effective exposure of the longer species to water [3]. Since we are mainly concerned with the case where d_P is close to the hydrophobic acyl chain length in the fluid phase, we need only consider a value of γ_{mis}^{LP} which describes the exposure of acyl chains (rather than protein side chains) to water. As described in Ref. 11 we therefore choose $\gamma_{mis}^{LP} = \gamma_{mis}^{LL} = 5 \cdot 10^{-16}$ erg/Å.

The total microscopic interaction energy is then obtained by adding Eqns. 1 and 2

$$\mathscr{H} = \mathscr{H}_{LL} + \mathscr{H}_{LP} \tag{3}$$

The only model parameter which so far has not been fixed is the direct lipid–protein interaction constant, J_{LP}, which is the only free interaction parameter of the present model study. The actual value of J_{LP} will depend on the properties of the protein hydrophobic surface, i.e., the type of amino-acid side chains. The possible values of J_{LP} will be discussed in Section III.

Calculational techniques

Monte Carlo computer-simulation techniques [8] offer a numerical way to derive the thermodynamic properties of the microscopic interaction model introduced above using the principles of statistical mechanics. Use of these numerical techniques ensures that the density fluctuations are accurately accounted for, and that the full entropy of mixing is included in the description. From the statistics we calculate the specific heat, $C(c,T)$, as a function of temperature for different protein molar fractions, c. c denotes the fraction of lattice sites occupied by proteins. Conventional Monte Carlo simulation only permits determination of derivatives of the free energy, such as the specific heat, and not the free energy itself [8]. We have therefore taken advantage of recently proposed methods [15–17] to analyze the simulation data which lead to that part of the free energy required to derive the phase equilibria. The technical aspects of applying these new methods to lipid-membrane phase transitions have recently been described by Zhang et al. [11]. Therefore we only give a brief description of the approach as applied to lipid/protein mixtures.

The conventional Monte Carlo simulations on the model of Eqn. 3 lead to a determination of a series of microconfigurations for the system which are characteristic of equilibrium at the thermodynamic conditions chosen. For a binary mixture these conditions are given by the value of the temperature, T, and the chemical potential, μ, of the proteins in the lipid-bilayer matrix. The chemical potential controls the equilibrium composition of the mixture given by the molar fraction of proteins, c. The total number of molecules in the mixture, i.e., the number of sites of the related lattice, is taken to be N. Now the molecular composition of the system fluctuates over the microconfigurations of the equilibrium ensemble. We can thus use the ensemble of microconfigurations generated at equilibrium to calculate the distribution function, $n(c,\mu,T,N)$, for the composition. Here $n(c,\mu,T,N)$ denotes the probability of occurrence of a microconfiguration with composition c at the values chosen for μ and T. Note that the distribution function is dependent on system size. The part of the free energy which describes the composition dependence of the total free energy for a fixed value of T, μ, and system size N [15,16] is related to $n(c,\mu,T,N)$ as follows

$$\mathscr{F}(c,\mu,T,N) = -\ln n(c,\mu,T,N) \tag{4}$$

The relative stability of two different membrane phases characterized by compositions $c^{(1)}$ and $c^{(2)}$ can now be determined by examining free-energy differences such as

$$\Delta\mathscr{F}(N) = \mathscr{F}(c^{(1)},\mu,T,N) - \mathscr{F}(c^{(2)},\mu,T,N) \tag{5}$$

Similarly, at phase coexistence, $\mu = \mu_m$, where the free energy will develop two pronounced, equally-deep minima corresponding to the two phases, the height of the barrier in free energy between the two phases can be determined as

$$\Delta\mathscr{F}(N) = \mathscr{F}(c_{max},\mu_m,T,N) - \mathscr{F}(c_{min},\mu_m,T,N) \tag{6}$$

where c_{max} and c_{min} denote the positions of the free-energy maximum and minimum, respectively. The barrier height in Eqn. 6 at coexistence (first-order transition) will scale as an interfacial free energy (interfacial tension), i.e.,

$$\Delta\mathscr{F}(N) \sim N^{1/2} \tag{7}$$

for a two-dimensional system. It is therefore possible to determine the phase boundaries for the system by locating minima in $\mathscr{F}(N)$ which are equally deep, i.e., $\Delta\mathscr{F}(N) = 0$ in Eqn. 5. The matching of the two minima is performed by studying $\mathscr{F}$ for varying μ. This is a sensitive procedure and is facilitated by use of the Ferrenberg-Swendsen reweighting technique [17] which allows us to calculate the distribution at a given value of μ using the data for the distribution function determined at a nearby value. From the size-dependence of

$\mathcal{F}(N)$ it is possible to locate the critical mixing point as the temperature where the barrier height, $\Delta\mathcal{F}(N)$ in Eqn. 6, no longer increases with system size but approaches a constant as the system size is increased. Beyond the critical point the barrier vanishes with increasing system size. These numerical methods, which have been developed to study the nature of phase transitions in one-component systems [15,16] and which here for the first time are being used to determine actual phase coexistence in two-component systems, are expected to provide very accurate results for the position of the phase boundaries. Recently, the same methods have been used to calculate phase equilibria in binary lipid mixtures (Zhang, Z., unpublished work).

III. Results

In this section we present simulation results for the model of a lipid–protein bilayer as described by the Hamiltonian of Eqns. 1–3. The geometric parameters of the protein are chosen to be $A_P = 68.0$ Å^2 and $d_P = d_{10} = 11.25$ Å, where d_{10} is the acyl-chain length in the fluid state. In most of the simulations we have chosen the direct lipid–protein interaction parameter to be $J_{LP} = 0.25 \cdot 10^{-13}$ erg. The results are derived from simulations using several different system sizes, $N = L \times L$, subject to periodic boundary conditions.

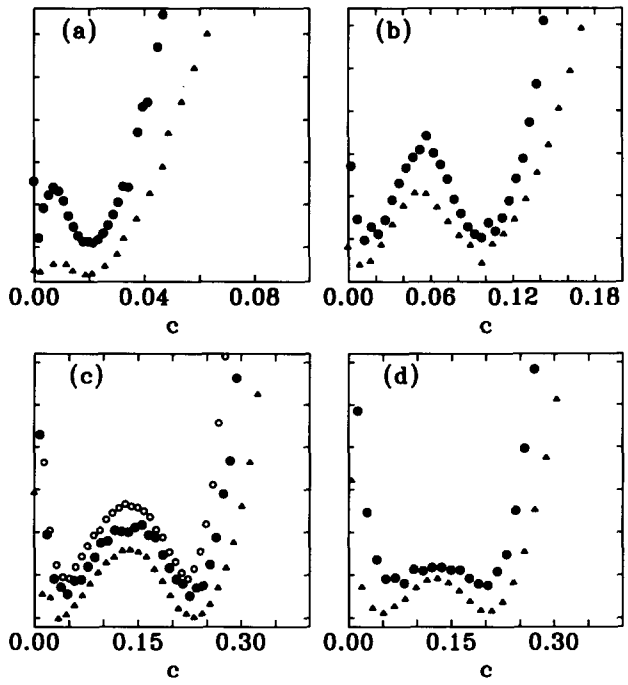

Fig. 1. Free energy $\mathcal{F}(c,\mu_m(N),T,N)$ as a function of membrane composition, c, for different lattice sizes, $N = L \times L$, $L = 16$ (△), 24 (●), 32 (○), for three different temperatures, (a): $T = 313.0$ K, (b): $T = 310.0$ K, (c): $T = 304.0$ K, and (d): $T = 303.5$ K. $\mu_m(N)$ refers to the chemical potential at phase coexistence for a system of size N consisting of a DPPC lipid bilayer embedded with small transmembrane proteins or polypeptides.

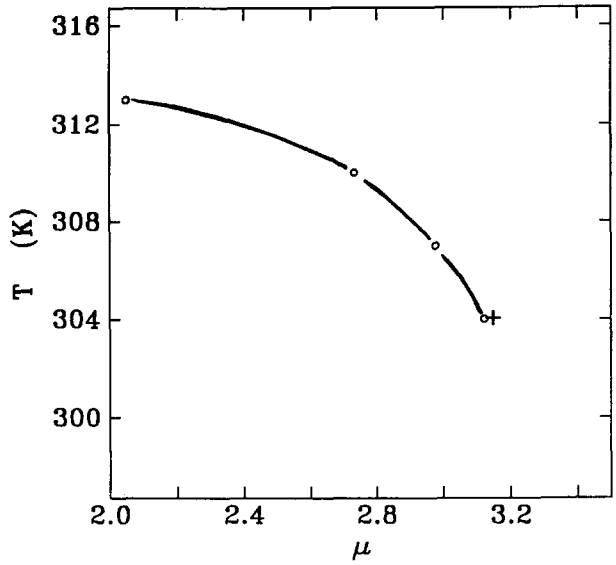

Fig. 2. Theoretical $T-\mu$ phase diagram for the microscopic model of lipid–protein interactions in Eqns. 1–3. The lower critical mixing point is marked by +. The diagram corresponds to a DPPC lipid bilayer embedded with small transmembrane proteins or polypeptides.

Very long simulations are performed at the chemical potential corresponding to the transition at the chosen temperature.

Fig. 1 shows the free energy function, $\mathcal{F}(c,\mu_m,T,N)$, for four different temperatures, $T = 313.0$ K, 310.0 K, 304.0 K, and 303.5 K, all of which are below the pure DPPC lipid-bilayer gel–fluid phase transition temperature, $T_m = 313.7$ K, of the present model. The free energy is presented for a value of the chemical potential, $\mu = \mu_m$, at which the two lipid phases are at coexistence and hence the two minima of the free energy are equally deep. At coexistence, the chemical potential of the proteins has the same value in the two phases. It should be noted that the free-energy functions in Fig. 1 not only represent the free energy of mixing but also contains the proper enthalpic part reflecting the non-ideality of the mixture. From the size dependence of the data in Fig. 1 the following conclusions can be drawn. For the two higher temperatures, $T = 313.0$ K and 310.0 K, the free-energy barrier, $\Delta\mathcal{F}(N)$ in Eqn. 6, separating the two minima increases with system size indicating that the two phases are separated by a first-order transition, i.e., the two phases coexist in the thermodynamic limit. In contrast, at $T = 304.0$ K in Fig. 1c, the barrier height does not depend on system size within the numerical accuracy indicating that the system is close to a continuous transition, i.e., in this case a lower critical mixing point. For even lower temperatures, e.g., $T = 303.5$ K in Fig. 1d, the barrier decreases with system size indicating that the difference between the two minima, and hence the two phases, vanishes in the thermodynamic limit.

At these temperatures the mixture is therefore in a one-phase region at all compositions.

The phase diagram spanned by temperature and chemical potential as obtained from data of the type presented in Fig. 1 is shown in Fig. 2. The solid line in this figure indicates the line of coexistence between the gel and fluid lipid phases. The line terminates in the critical mixing point.

The corresponding phase diagram spanned by temperature and membrane composition is displayed in Fig. 3. This figure shows that the lipid–protein interactions of the present microscopic model produce the characteristic 'tear-drop'-shaped closed coexistence loop of a binary mixture with a lower critical mixing point. For larger values of the direct lipid–protein interaction constant, J_{LP} in Eqn. 2, the critical mixing point moves towards higher temperatures as expected.

In Fig. 4 are shown selected specific-heat scans for a series of temperatures both for the pure DPPC bilayer, within the coexistence region, close to the critical mixing point, and beyond criticality. The data show that the endothermic transition peak for the pure system is broadened progressively as the protein is incorporated in larger concentrations. It is seen that a broad shoulder develops at the low-temperature side and that the large peak broadens and loses intensity and moves towards lower temperatures. All these signals weakly reflect the underlying phase diagram in Fig. 3. It is observed that the solidus line leaves no apparent feature in the specific heat. It is particularly noteworthy that the wings of the specific heat function increase in intensity as the protein is incorporated implying that the fluctuations in the mixed system are enhanced.

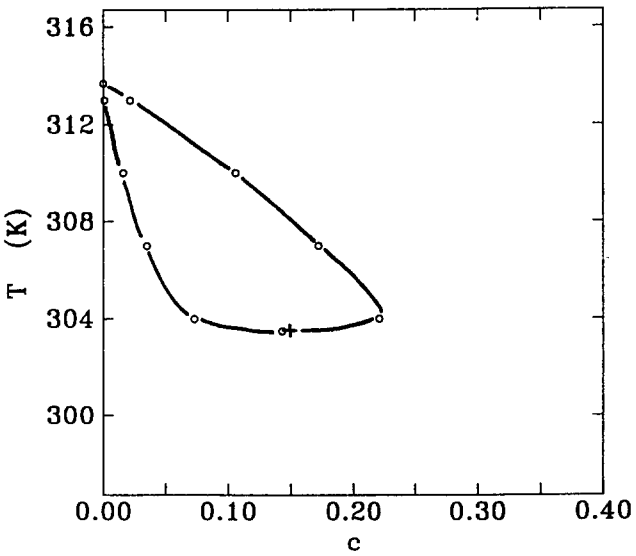

Fig. 3. Theoretical $T-c$ phase diagram (o) for the microscopic model of lipid–protein interactions in Eqns. 1–3. The solid curve is drawn as a guide to the eye. The critical mixing point is indicated by +. The diagram corresponds to a DPPC lipid bilayer embedded with small transmembrane proteins or polypeptides.

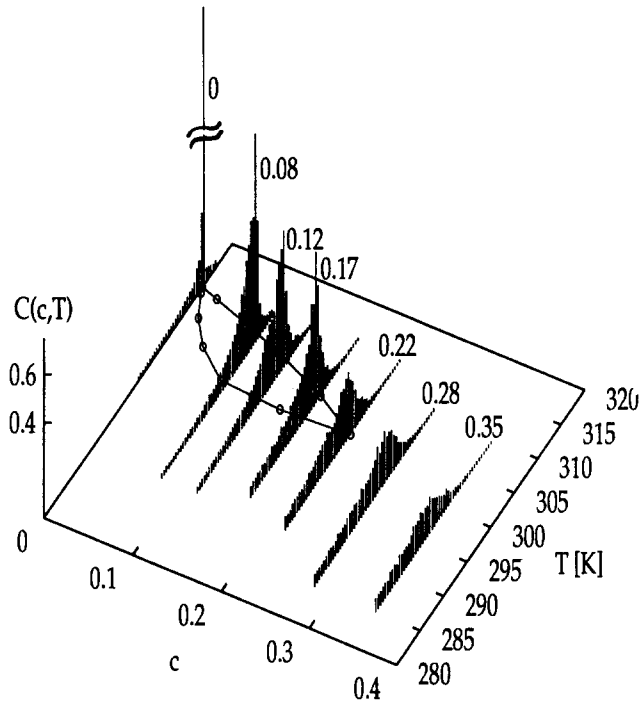

Fig. 4. Specific-heat traces as a function of temperature for the microscopic model of lipid–protein interactions in Eqns. 1–3 shown for a system of size $N = 60 \times 60$ for a series of different protein concentrations, c. The data correspond to a DPPC lipid bilayer embedded with small transmembrane proteins/polypeptides. The theoretical phase diagram of Fig. 3 is shown in the $c-T$ plane.

These fluctuations are pronounced close to the critical mixing point. Finally we note that a specific-heat peak remains even beyond the critical point. Hence, the local composition in the mixture in this region, which is a thermodynamic one-phase region, is strongly fluctuating. It should be remarked that the peak in the specific heat which persists beyond the coexistence region contains a non-zero amount of heat which, however, does not correspond to a transition enthalpy. We shall return to the transition enthalpy in the following section.

IV. Comparison with experiments

The occurrence of critical mixing in two-component lipid membranes is likely to be a wide-spread phenomenon. There is strong experimental evidence that it occurs in DMPC and DPPC lipid bilayers mixed with either gramicidin A [7] or with synthetic transmembrane amphiphilic polypeptides of the type Lys_2-Gly-Leu_n-Lys_2-Ala-amide with $n = 16$ and 24 [5,6,9]. The phospholipid/polypeptide systems have been studied using a combination of calorimetry and NMR difference spectroscopy and the resulting phase diagrams have a high degree of accuracy. The experimental data for the phospholipid/gramicidin A system have not yet been interpreted in terms of a quantitative phase diagram although it has been argued that the data are

consistent with the presence of a lower critical mixing point [7]. Since there may also be some influence of the dimer-monomer equilibrium in the case of gramicidin A which we have not accounted for in the present type of modelling, we shall restrict ourselves to a quantitative comparison of our theoretical results on critical mixing with DPPC lipid bilayers incorporated with the synthetic polypeptides. Since the experimental data for both the long and the short peptide are quite similar, we discuss these two systems together. It should however be noted that there is a slight quantitative difference between the phase diagram for the two peptides which can easily be rationalized in terms of the hydrophobic matching concept. The short peptide tends to stabilize the fluid phase more strongly than the long peptide because the short peptide is more closely matched to the fluid hydrophobic thickness of DPPC than the long peptide [1].

The simulation data for the specific-heat traces in Fig. 4 show that the phase boundaries in the phase diagram in Fig. 3 do not manifest themselves in strong anomalies. In particular, the position of the solidus line cannot be inferred directly from the shape of the specific heat. This underscores the point made in the

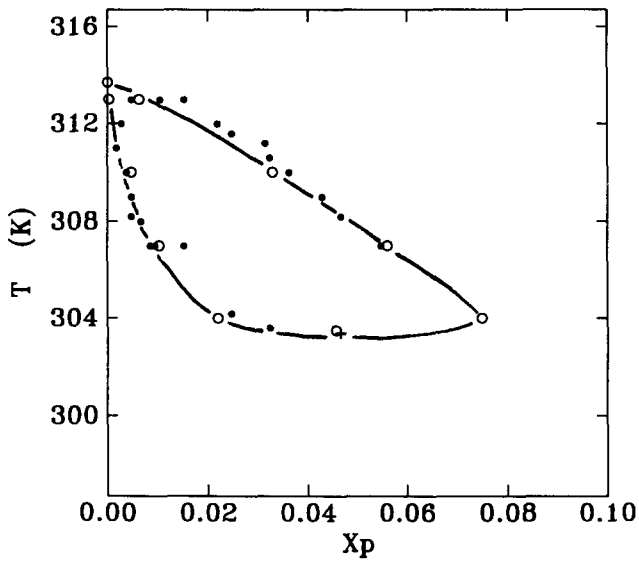

Fig. 5. Rescaled theoretical $T-x_P$ phase diagram (○) for the microscopic model of lipid–protein interactions in Eqns. 1–3. The rescaling is performed in order to facilitate a comparison with a specific membrane system: DPPC bilayers mixed with α-helical amphiphilic transmembrane proteins of the type Lys_2-Gly-Leu_n-Lys_2-Ala-amide. The experimental data (●) for mixtures of DPPC with Lys_2-Gly-Leu_{16}-Lys_2-Ala-amide [6] are shown for comparison. The solid line connecting the theoretical points is drawn as a guide to the eye. The experimental phase diagram for the longer peptide with $n = 24$ is very similar [6]. Note, that since the experiments have been carried out on perdeuterated DPPC which has a lower transition point than that of normal DPPC, the experimental data have been subject to a trivial translation in temperature in order to compensate for the isotope effect and to facilitate the comparison between theory and experiment.

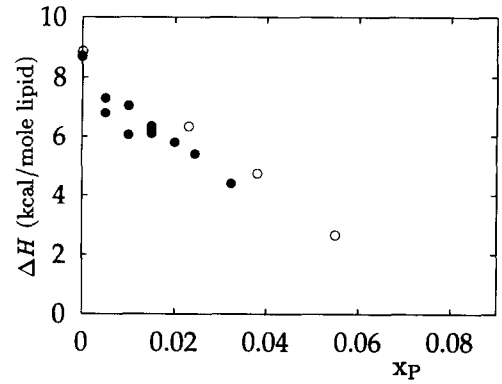

Fig. 6. Transition enthalpy, ΔH per mole lipid, as a function of peptide concentration, x_P, as obtained from theoretical calculations on the microscopic model (○) of lipid–protein interactions in Eqns. 1–3 and from calorimetric measurements on DPPC bilayers mixed with α-helical amphiphilic transmembrane proteins of the type Lys_2-Gly-Leu_{16}-Lys_2-Ala-amide (●) [6]. The theoretical data have been scaled to the experimental value of ΔH for the pure DPPC bilayer.

Introduction that great care must be taken when using derivatives of the free energy to determine phase equilibria. This is particularly true close to critical points where the fluctuations lead to pronounced wings in the specific heat function and where a substantial peak in the specific heat is present even beyond the critical point where there is no transition, cf. Fig. 4. There are several examples in the literature where such apparent specific-heat anomalies have incorrectly been taken as indications of a phase transition or a phase-coexistence region. The family of specific-heat traces across the phase diagram for the present model system shown in Fig. 4 is in close qualitative agreement with experimental DSC measurements for the DPPC/polypeptide system [6].

In order to make a direct quantitative comparison between the theoretical phase diagram in Fig. 3 and the corresponding experimental data, it is first necessary to scale the theoretical data in a manner which allows for the fact that the peptides in the experimental system are larger relative to the lipid acyl-chains than assumed in the lattice model of Eqns. 1–3. In the model description it was assumed for computational convenience that the peptides are single-site objects on the lattice substituting for a single acyl chain. Although it is in principle feasible, it would be computationally more demanding to perform the simulation with objects which occupy several adjacent lattice sites. It is however possible to scale the data in Fig. 3 to provide an approximation to the case where the polypeptides occupy more sites and hence have a larger volume fraction. The approximation underlying this simple scaling is on the same level as the Flory-Huggins approximation for polymer blends which for the present system overestimates the mixing entropy. For concentrations which are not too high this approximation

should be reliable. Fig. 5 shows the same data for the phase diagram as in Fig. 3 but now scaled down to a concentration measure, x_P, corresponding to a polypeptide which occupies seven lattice sites appropriate for a polyleucine α-helix, i.e., $x_P = c((7/2) - (5c/2))^{-1}$. For comparison we have plotted on the same figure the experimental data for the DPPC/polypeptide membrane as obtained for NMR difference spectroscopy [5]. A further comparison with experimental data is performed in Fig. 6 where calorimetric data [6] for the transition enthalpy per mole lipid, $\Delta H(x_P)$, are shown together with the data obtained from the simulations on the microscopic model. The agreement between the experimental data and the theoretical predictions for the phase diagram and the variation of transition enthalpy with polypeptide concentration are quite satisfactory considering the approximation which underlies the concentration scaling. The good agreement suggests that the microscopic interaction model has captured the essentials of the lipid–protein interactions in the present membrane system. Specifically it suggests that the direct lipid–protein interactions are responsible for the location of the critical mixing point.

A remark is pertinent in relation to the concentration dependence of the transition enthalpy shown in Fig. 6. ΔH goes strictly to zero at the terminus of the coexistence loop, even though the specific heat in this region still has a peak with a finite content of heat, cf. Fig. 4. This amount of heat does not correspond to a transition enthalpy. The intercept of ΔH with the concentration axis carries no particular microscopic significance and should not be related to a lipid annulus or an amount of lipid molecules 'removed' from the transition.

Finally, we wish to point out that the succesful use of the hydrophobic-matching concept in the modelling of lipid–protein and lipid–polypeptide interactions and its consequences for lipid-membrane phase equilibria should definitely be useful for the modelling of more complex membrane systems, such as ternary mixtures of lipids, polypeptides, and cholesterol. It was recently shown in an experimental NMR study by Nezil and Bloom [18] that the cholesterol-induced thickening effect on fluid lipid bilayers can be counteracted by a compensating thinning effect of short synthetic polypeptides in accord with the predictions of the hydrophobic-matching criterion. It would therefore be of interest to extend both the experimental and the theoretical work discussed in the present paper to such three-component systems in order to gain further insight into the nature of lipid–protein interactions in membranes.

Acknowledgements

This work was supported by FCAR du Quebec under a centre and team grant and by the Danish Natural Science Research Council under Grant No. 11-7785.

References

1 Mouritsen, O.G. and Sperotto, M.M. (1992) in Thermodynamics of Membrane Receptors and Channels (Jackson, M., ed.), pp. 127–181, CRC Press, Boca Raton, Florida.
2 Watts, A. (ed.) (1993) Protein–Lipid Interactions, New Comprehensive Biochemistry, Elsevier, Amsterdam, in press.
3 Mouritsen, O.G. and Bloom, M. (1984) Biophys. J. 46,141–153.
4 Mouritsen, O.G. and Bloom, M. (1993) Annu. Rev. Biophys. Biomol. Struct. 22, 147–171.
5 Huschilt, J.C., Hodges, R.S. and Davis, J.H. (1985) Biochemistry 24, 1377–1386.
6 Morrow, M.R., Hushilt, J.C. and Davis, J.H. (1985) Biochemistry 24, 5396–5406.
7 Morrow, M.R. and Davis, J.H. (1988) Biochemistry 27, 2024–2032.
8 Mouritsen, O.G. (1990) in Molecular Description of Biological Membrane Components by Computer Aided Conformational Analysis, Vol. 1 (Brasseur, R., ed.), pp. 3-83, CRC Press, Boca Raton, FL.
9 Morrow, M.R. and Whitehead, J.P. (1988) Biochim. Biophys. Acta 941, 271–277.
10 Pink, D.A. and Chapman, D. (1979) Proc. Natl. Acad. Sci. USA 76, 1542–1546.
11 Zhang, Z., Laradji, M., Guo, H., Mouritsen, O.G. and M.J. Zuckermann (1992) Phys. Rev. A 45, 7560–7567.
12 Pink, D.A., Green, T.J. and Chapman, D. (1980) Biochemistry 19, 349–356.
13 Sperotto, M.M. and Mouritsen, O.G. (1991) Eur. Biophys. J. 19, 157–168.
14 Sperotto, M.M. and Mouritsen, O.G. (1991) Biophys. J. 59, 261–270.
15 Lee, J. and Kosterlitz, J.M. (1990) Phys. Rev. Lett. 65, 137–140.
16 Lee, J. and Kosterlitz, J.M. (1991) Phys. Rev. B 43, 3265–3277.
17 Ferrenberg, A.M. and Swendsen, R.H. (1988) Phys. Rev. Lett. 61, 2635–2638.
18 Nezil, F.A. and Bloom, M. (1991) Biophys. J. 61, 1176–1183.